OXFORD

Cerebral Cortex, 2025, **35**, bhaf203
https://doi.org/10.1093/cercor/bhaf203
Advance access publication date 2 August 2025
Original Article

Activity of CaMKII-expressing neurons in medial prefrontal cortex of male and female Long-Evans rats is necessary for encoding odor information and novelty recognition in an odor-based incidental memory test

Ilne L. Barnard[1], Dan L. McElroy[1], Kaylen M. Young[1], Dylan J. Terstege[2,3], Aiden E. Glass[1], Jonathan R. Epp[2,3], Justin J. Botterill[1], and John G. Howland[1,*]

[1]Department of Anatomy, Physiology, and Pharmacology, University of Saskatchewan, Health Sciences Building, 107 Wiggins Rd, Saskatoon, SK S7N 5E5, Canada
[2]Department of Cell Biology & Anatomy, University of Calgary, Cumming School of Medicine, HMRB 212, 3330 Hospital Drive NW, Calgary, AB, T2N 4N1, Canada
[3]Hotchkiss Brain Institute, University of Calgary Foothills, 3330 Hospital Dr NW, Calgary, AB T2N 4N1, Canada

*Corresponding author: John G. Howland, Department of Anatomy, Physiology, and Pharmacology, University of Saskatchewan GD30.7, Health Sciences Building 107 Wiggins Road Saskatoon, SK S7N 5E5. Canada. Email: john.howland@usask.ca

Incidental memories encoded through spontaneous interaction with stimuli in an environment contribute to higher cognitive functions. The spontaneous Identical (IST) and the Different Stimuli Tests (DST), with objects and odors, allow for incidental memory testing using variable memory loads in rats. Here, fiber photometry and chemogenetics were used to examine the necessity of CaMKII-expressing neurons in medial prefrontal cortex (mPFC) for novelty discrimination in the IST and DST with odors. Male and female Long Evans rats completed 6-odor IST and DST. No differences in total exploration times or stimuli visits were observed in either test or sex. During the sample phase of the DST, a heightened response and a sustained increase in mPFC neuronal activity occurred during the first stimulus interaction. A sustained increase in mPFC neuronal activity during interaction with the novel stimulus was also observed in the test phase of the DST, but not the IST. Activation of inhibitory DREADDs expressed in mPFC CaMKII-expressing neurons impaired novelty preference in the DST, but not IST, and significantly decreased c-Fos + cells in the mPFC. Taken together, we show increased activity in mPFC CaMKII-expressing neurons facilitates novelty recognition under higher memory loads in the DST.

Significance statement
Odors are an important element of memory and can carry great emotional significance. However, the neural substrates supporting odor-based novelty recognition are not yet well understood. We show that an increase in activity of CaMKII-expressing neurons in the mPFC facilitates novelty recognition in a spontaneous odor recognition test with seven but not two unique stimuli. These results suggest that increased test complexity engages the mPFC, resulting in encoding of the novel stimulus and coordinated odor-based attention among odors. Then, the mPFC may coordinate novelty-driven behavior manifested as increased interaction with novel stimuli. These findings contribute to our understanding of the circuitry underlying odor recognition memory, which may relate to odor-based memory deficits in individuals with neurodegenerative and neuropsychiatric diseases.

Keywords: medial prefrontal cortex; novelty recognition; odor; fiber photometry; c-Fos.

Introduction

Many of our day-to-day experiences enter memory without explicit intention. These incidental memories are encoded through spontaneous interaction and exploration in an environment (Wagnon et al. 2019; Torromino et al. 2022). Incidental memory capacity refers to the limited nature of spontaneous memory encoding and may be influenced by stimulus type, cognitive engagement (i.e. attention), or environmental complexity (Broadbent et al. 2004; Barch and Smith 2008; Sannino et al. 2012; Torromino et al. 2022). Once encoded, incidental memories can form and/or influence the memory representations of events or stimuli being held in working memory. Considering that incidental and working memory deficits are prevalent in individuals with neurodegenerative and neuropsychiatric disorders, a greater understanding of the underlying circuitry is essential to understanding disease progression and prognosis and would aid the development of better treatment strategies (Unsworth 2016; Wagnon et al. 2019).

Spontaneous object-based recognition tests like novel object recognition (NOR), Object-in-Place (OiP), and temporal order memory (TOM) are widely used in rodents to study incidental memory (Ennaceur 2010; Warburton and Brown 2015; Aggleton

Received: March 20, 2025. **Revised:** June 26, 2025. **Accepted:** July 1, 2025

and Nelson 2020; McElroy et al. 2024). Recent development of the spontaneous Identical Stimuli Test (IST) and the Different Stimuli Test (DST), with both objects and odors, allows for load-dependent incidental memory testing to occur in an efficient, sophisticated, and cost-effective manner in rats (Ennaceur and Delacour 1988; Ennaceur and Aggleton 1994; Broadbent et al. 2004; Barnard et al. 2023) and mice (Broadbent et al. 2010; Sannino et al. 2012; Olivito et al. 2016; Olivito et al. 2019; Torromino et al. 2022). These tests rely on rodents' innate novelty seeking behavior, shown by preferential interaction with the novel stimulus after a 1-min delay (Barnard et al. 2023). In the IST, rodents are presented with a set of incidental stimuli in the sample phase, whereas in the DST, rodents interact with a set of different stimuli, allowing for testing under a low- and high-memory load, respectively.

Rats have considerable olfactory learning and memory capabilities because their primary sense is olfaction, which supports increased sensitivity in odor-based memory tasks (Eichenbaum and Robitsek 2009). Odor-based memory is primarily studied in reward-driven and rule-based tasks, like the odor span task (Farovik et al. 2008; Davies et al. 2013; De Falco et al. 2019; Scott et al. 2020). Use of these odor-based operant conditioning tasks has shown the mPFC is critical for working memory (Farovik et al. 2008; Davies et al. 2013; Scott et al. 2020). However, the underlying circuitry of odor-based incidental memory has not yet been fully delineated in spontaneous tests like the IST and DST with odors, specifically non-social odors. Social odors are often used in recognition memory paradigms, and the mPFC plays a role in these tests (Robinson et al. 2019). As well, it has been demonstrated that the mPFC facilitates odor-directed attention, to aid in encoding odor memories in paradigms using social odors (Cansler et al. 2023). Further, the mPFC has connections to and from the primary olfactory cortices, including the anterior olfactory nucleus, taenia tecta, the orbitofrontal cortex, and the piriform cortex, which all play a role in processing olfactory information (Cansler et al. 2023). Lastly, the mPFC also projects to and from the perirhinal cortex (Bussey et al. 2006; Feinberg et al. 2012) and entorhinal cortex (Persson et al. 2022), which are critical for 2-item odor-based recognition memory. In the present experiments, we used non-social odors to directly investigate the role of the mPFC in odor-based incidental memory. We hypothesized that by using six unique non-social odors in the DST, a more complex odor profile will be presented than in the IST with odors, which would engage the mPFC in the test. We also closely measured the rats' behavior during the test by examining interaction times, number of visits to the stimuli, and if any sex differences were present. We demonstrate here using fiber photometry a sustained increase in mPFC neuronal activity during interaction with a novel stimulus under higher memory loads in the test phase of the DST with odors. We also observed novelty preference deficits under higher memory loads of the DST with odors following inhibitory DREADD activation in the mPFC in both sexes. No differences in exploration times or visits to stimuli exist with an increase in interaction time during the DST with odors. These results suggest that mPFC is a critical component of the circuitry underlying odor recognition in odor rich environments.

Materials and methods

Subjects and experimental design

Adult (2–4 months of age) male and female Long-Evans rats ($n = 26$/sex; Charles River Laboratories, Kingston, NY) were pair housed in a vivarium (12-h light/dark cycle, lights on at 0700) in standard ventilated cages with ad libitum water and food, and a plastic tube for environmental enrichment. In an initial experiment, 18 rats (9 per sex) were used to measure calcium transients with fiber photometry in the mPFC during both the IST and DST with odors (4 total tests/rat). In a second experiment, possible off-target effects of Compound 21 (C21) were investigated using six naïve male and female rats (12 total) that completed the IST and DST with odors following an i.p. injection of saline or 1 mg/kg C21 (4 total tests/rat). In a third experiment, 12 male and female rats (24 total) underwent vector infusions into the mPFC, then performed both the IST and DST with odors after an i.p. injection of saline or 1 mg/kg C21 (4 total tests/rat). The order of tests was quasi-counterbalanced and rats had a week washout period between tests in all experiments. In a fourth experiment, 16 rats (8 per sex) expressing the active vector in the mPFC were used to evaluate the expression of c-Fos in the mPFC. These rats completed the DST with odors after an i.p. injection of saline or of 1 mg/kg C21 before being perfused 90 min after testing. All procedures followed guidelines from the Canadian Council on Animal Care and were approved by the University of Saskatchewan Animal Research Ethics Board.

Vectors and drug treatment

Adeno-associated viruses (AAVs) were bilaterally infused into the mPFC. An AAV9-CamKIIa-jGCaMP8m-WPRE (2.7×10^{13} vg/ml, Addgene #176751; 18 rats (9/sex) vector was used in experiment 1 for fiber photometry. Control vectors were AAV5-CaMKIIa-GFP (1.9×10^{13} vg/ml, Addgene #50469; four rats (2/sex) in experiment 2) and AAV5-CaMKIIa-mCherry (3×10^{12} vg/ml, Addgene #50477; four rats (2/sex) in experiment 2). The active inhibitory DREADD vector used was AAV5-CaMKIIa-hM4D(Gi)-mCherry (2.4×10^{13} vg/ml, Addgene #50477). The inhibitory DREADD agonist C21 dihydrochloride (water soluble) (1 mg/kg, HelloBio HB6124), was delivered via an i.p. injection 1 h prior to behavioral testing. Doses between 0.5–1 mg/kg of C21 are often used in the literature with sufficient efficacy and minimal off-target effects (Du et al. 2022; Miranda et al. 2022; Jendryka et al. 2019; Thompson et al. 2018).

Stereotaxic surgery protocol

Rats underwent stereotaxic surgery using previously established procedures (Botterill et al. 2021; Botterill et al. 2024; McElroy et al. 2024). Rats were anesthetized with the inhalant anesthetic isoflurane (Janssen) and their heads were shaved. After the rat was positioned in a stereotaxic apparatus, tear gel (Bausch + Lomb) was applied to each eye, and their head was swabbed with Chlorhexidine gluconate solution with 4% v/v isopropyl alcohol and iodine. A 3 ml saline injection was given in each flank of the leg, and an injection of slow-release buprenorphine HCL (0.6 mg/kg, Chiron) was given subcutaneously. Body temperature was monitored throughout with a homeothermic monitor (Harvard Apparatus), and heartrate and blood oxygen saturation were monitored throughout using a pulse oximeter. Following anesthesia and preparation, the scalp was cut and retracted to expose the dorsal surface of the skull. Holes were drilled at the following coordinates for the mPFC: AP + 3.2 mm, ML ±0.5mm. Virus was then delivered using a 1.0 μl Neuros Syringe (Hamilton, Model 7001 KH, 32 gauge, Point Style 4) attached to a probe holder on the stereotaxic apparatus. The syringe was lowered to a DV of—4 mm from bregma for the mPFC. A total of 0.65 μl was injected into each hemisphere at a rate of 0.20 μl per min (Timme et al. 2022). The needle was left in place for 1 min was then lifted 0.25 mm for an additional 4 min. For experiment 1, a 4.75 mm

fiber optic cannula (Neurophotometrics) was then inserted to a DV of −3.85 following the viral infusion. The cannula was secured using four surgical screws and dental acrylic. For experiments 2 and 3, following the completion of the viral injections, bone wax was carefully placed over the craniotomies, and the wound was cleaned with Chlorhexidine Acetate Ointment (Inhibit). The scalp was then sutured with PDS II 3–0 violet filament, with a 3/8″ cutting needle (Ethicon, Z452). All rats were placed in a clean cage on top of a heating pad for recovery from surgery. Rats were monitored daily following surgery, and testing began 3 weeks later.

Apparatus and testing materials

Apparatus, testing materials, and procedures closely followed our previous protocols (Barnard et al. 2023). Rats were handled in the testing room (3 min a day for 3 d) and then habituated to the testing apparatus (10 min for 2 d). Rats in experiment 1 were also habituation to the fiber photometry system. Behavioral testing occurred in white corrugated plastic boxes (60 cm × 60 cm × 60 cm) with the stimuli evenly presented between two opposing walls at three positions (9 cm from side of box, 21.5 cm apart from each other). Odor stimuli were created using 250 ml glass canning jars with nine holes drilled in the lids of the jars to allow rats to smell the odors. The jars were filled with sand for stability and to provide a platform for a small plastic vial (Fisherbrand scintillation vials, 18 ml) filled half-way with a powered household spice (lemon pepper, dill, sage, onion, anise, cloves, ginger, cumin, cocoa, celery salt, coffee, cinnamon, garlic, or oregano). Odor jars were affixed to the testing box with Velcro™.

Spontaneous incidental memory test protocol

On the test day, the box was prepared with the first set of stimuli for the particular test taking place. The rat was then placed into the box for the sample phase (5 min), taken out, and placed inside their assigned transport cage for a 1-min delay. During the delay, all stimuli were replaced with new stimuli for the test phase. Then, the rat was placed back into the box for the 5-min test phase. After, the box and stimuli were cleaned with 70% ethanol. In the sample phase of the IST, a set of six identical odor stimuli were presented, then after the delay, a novel stimulus was introduced alongside five clean copies of the odor from the sample phase. In the DST, a set of six different odor stimuli were presented in the sample phase, and in the test phase, clean copies of the five odors from the sample phase were presented with one novel odor. The odors presented in each test, their positions, and the odor used for the novel stimulus were all randomized.

Behavioral videos for all experiments were recorded from an overhead perspective in full color at a frame rate of 30 fps and a resolution of 1080 pixels × 1080 pixels (Logitech Brio 505, Logitech). The entire video was then manually scored using a stopwatch, where the duration of interaction at each odor stimulus was recorded (Barnard et al. 2023). To increase accuracy of scoring, videos were watched at half speed using the media player IINA, and the interaction times were adjusted accordingly. Interaction was noted when the rat's nose was within 2 cm of the top of the odor jar, while looking at and/or chewing the stimuli for a duration longer than 50 ms. Videos were scored blinded to treatment, and a reliability check was confirmed with a second scorer on a subset of videos ($r(10) = 0.91$, $P = 0.00020$). Novelty recognition was measured using a discrimination ratio, where the time spent with the novel stimulus was compared to the average time spent with familiar stimuli (DR = [T (novel)—T (avg. familiars)/T (total)]. Positive discrimination ratios indicate a novelty preference.

Fiber photometry recordings

For experiment 1, a FP3002 Neurophotometrics system was used to record calcium fluorescence from the rat mPFC. A 470 nm excitation wavelength was used to image the green calcium indicator (GCaMP8m) and a 415 nm excitation wavelength was used for an interleaved isosbestic control for elimination of artifacts (i.e. calcium-independent signals). A Bonsai workflow (designed by Neurophotometrics) was used to record the fiber signals and generate a video of the behavior. Rats were connected to the fiber photometry system for the entire duration of the test session.

Fiber photometry analysis

Videos generated during this experiment were manually annotated to note each interaction with an odor stimulus, including the timestamp, duration, position, and type of stimulus. Then, the annotated files and raw photometry traces were imported and aligned by a custom MATLAB script (Terstege et al. 2023; https://github.com/dterstege/PublicationRepo/tree/main/Barnard2024). To start, the annotated behavior file and the fiber photometry output were uploaded to the script. Noise was filtered out of each signal trace and the isosbestic data was fit with a biexponential decay and scaled to the raw 470 nm data with a robust fit. This data was converted to a z-score ΔF/F and processed using a lowpass filter. A converted z-scored ΔF/F normalized the fluorescence signal to account for differences in baseline fluorescence differences between recordings, allowing the relative changes in the signals to be compared among the recordings. The photometry trace was then split into the defined sample and test phases, to examine the ΔF/F for the entire test segment. The timestamp of each interaction was used to generate the ΔF/F for each interaction bout. A minimum bout duration was set to 1 s, and the time examined prior to and after the interaction was set to 1 s. The peak detection criterion was set to 0.5 standard deviations. For each interaction, the area under the curve, peak z-score, peak frequency, mean peak height, and the dynamic range were generated. Subsequent data was analyzed using GraphPad Prism 10.2.2 software.

Histology, immunohistochemistry, and microscopy

Following behavioral experiments, rats were deeply anesthetized with isoflurane. Once unresponsive, they were transcardially perfused with 0.1 M phosphate-buffered saline (PBS) followed by 4% paraformaldehyde fixative (PFA). Brains were extracted and stored in 4% PFA for 24 h. Brains from experiment 1 and for the c-Fos analysis in experiment 4 were transferred to a 0.01% sodium azide in PBS solution until sectioned. These brains were sectioned at 50 um in the coronal plane using a vibratome (Leica VT1000 S). The remaining brains from experiment 3 were transferred to a 30% sucrose solution for 3 d prior to sectioning. These brains were sectioned at 50 um in the coronal plane using a cryostat (Leica SM 2000R). All sections were stored in a 60% glycerol solution at −20 °C.

To view the location, spread, and intensity of vector expression, sections were rinsed 3 times for 10 min in PBS and then stained with Hoechst Stain (1:2000 from stock, Cell Signaling Technology, 33,342). Sections were rinsed twice more for 5 min each before being mounted onto gelatin-coated microscope slides and left to airdry. Once dried, slides were coverslipped and imaged using a confocal microscope (LSM 700 laser scanning confocal microscope, Carl Zeiss) at 5X using the 405 (blue) and 594 (red) nm laser.

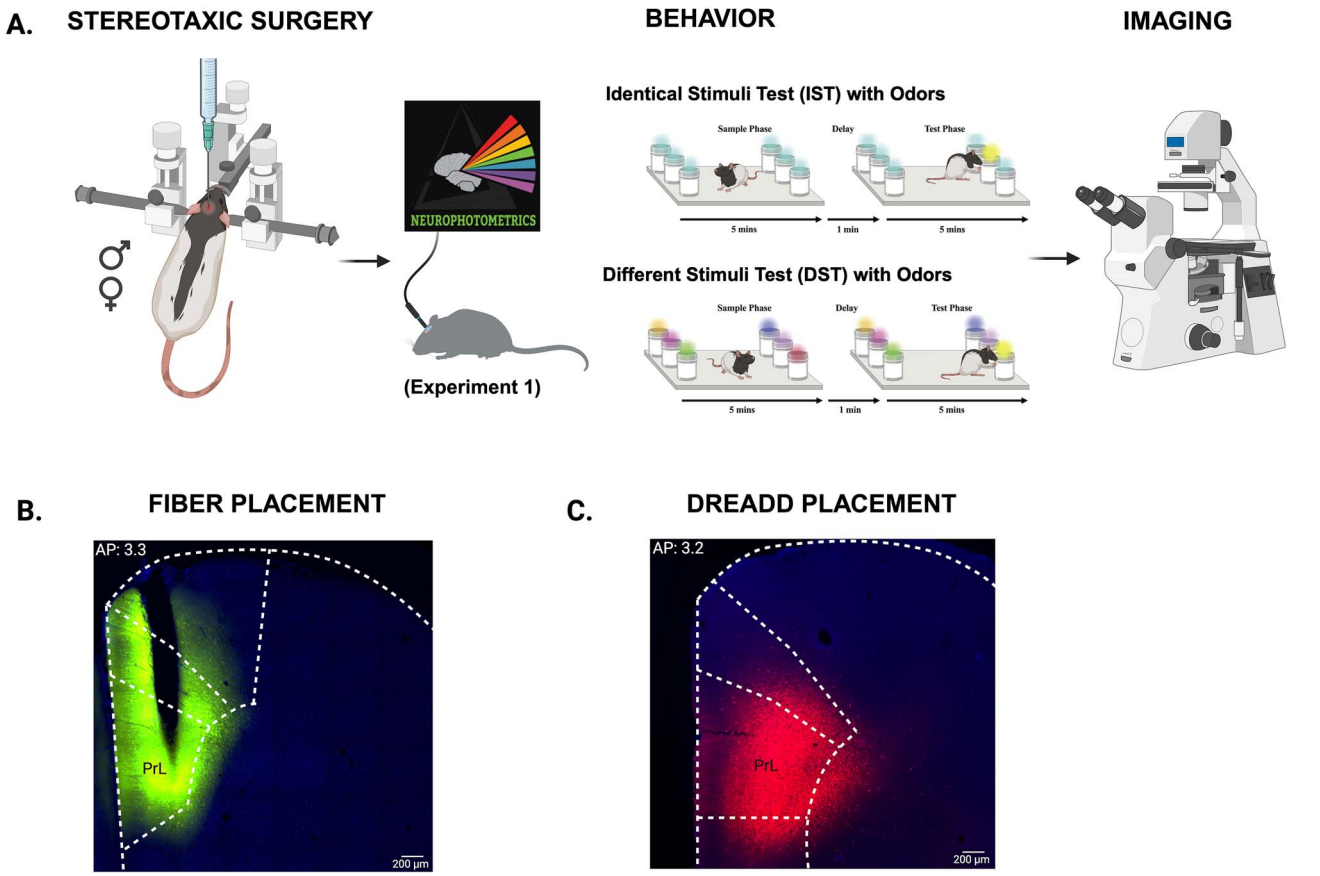

Fig. 1. Experimental design. (A). First, male and female rats underwent stereotaxis surgery. In experiment 1 the AAV9-CamKIIa-jGCaMP8m-WPRE vector was unilaterally infused into the prelimbic region of the mPFC [18 (9 per sex)]. In experiment 3, either a control (AAV5-CaMKII-GFP or AAV5-CaMKII-mCherry) or active vector (AAV5-CamKIIa-hM4D(Gi)-mCherry) was bilaterally infused into the prelimbic region of the mPFC [14 active (7 per sex), 10 control (5 per sex)]. Following a two-week recovery, the rats underwent behavioral testing. In experiment 1 calcium dynamics were recorded using fiber photometry and rats completed both the IST and DST with odors. In experiment 3, rats completed both the IST and DST with odors following either a saline or C21 *i.p.* injection (1.0 mg/kg) in a pseudorandom order. All brains were then sectioned using a cryostat or vibratome, and sections were stained with Hoescht. Lastly, a confocal microscope was used to image the brain sections to confirm the vector placement and expression. (B). An example of a brain from experiment 1 with adequate vector expression and location. (C). An example of a brain from experiment 3 with adequate vector expression and location. Images were taken using a confocal microscope at 5X using a 594 nm laser, and the prelimbic region of the mPFC (PrL) is labeled. Figure created with biorender.

To analyze c-Fos expression in the subset of 16 brains, sections were rinsed 3 times for 5 min in PBS, then twice for 5 min in PBSx (1x PBS + 0.3% Triton X 100). Sections underwent an hour of blocking in 5% Normal Goat Serum. Sections were incubated in TNB Buffer and 0.3% Triton X 100 with the mCherry primary (Rabbit anti-mCherry, Abcam, #167453, 1:3000) and c-Fos primary (Guinea Pig anti c-Fos, Synaptic Systems, #226308, 1:5000) antibodies for 24 h. The following day sections were rinsed in PBS twice for 10 min and then incubated in PBSx and mCherry secondary (Alexa Fluor 568 goat anti-rabbit IgG (H + L), Invitrogen by Thermo Fisher Scientific, #A-11011, intraperitoneal, 1:500) antibody for 1 h. Sections were rinsed in PBS for 5 min before incubating in TNB Buffer (TSA blocking reagent, 100 mM Tris, pH 7.5, 150 mM NaCl) and the c-Fos secondary (Alexa Fluor 488 goat anti-guinea pig, Invitrogen by Thermo Fisher Scientific, #A-11073; 1:1200) antibody. Finally, sections were rinsed twice for 5 min in PBS, stained with Hoechst Stain for 10 min, and rinsed twice more for 5 min in PBS. Sections were mounted onto gelatin-coated microscope slides and left to airdry before being coverslipped and imaged on the confocal microscope (Zeiss LSM700 laser scanning confocal microscope, Carl Zeiss) at 5X using the 405 (blue), 594 (red) and 488 (green) nm lasers. Representative images were taken on an epifluorescence microscope (Carl Zeiss Microscopy GmbH, Carl-Zeiss-Promenade 10. 07745 Jena) using water immersion on 25x to observe co-localization of c-Fos in DREADD-expressing cells and processed using Zen 3.9 Deconvolution Software. Only the rats with appropriate placement and vector expression were accepted for statistical analysis (Fig. 1B, C).

Image analysis

From each animal, 1–4 images (1024 × 1024 pixels) were taken of the target area. Using FIJI (Image J, Version 2.14.0/1.54f), the images taken from the three channels of the confocal microscope (405, 488, 555 nm) were merged into one composite image. Vector expression, location, and spread were then evaluated. On the subset of images that were stained for c-Fos (pseudocoloured green), a consistent region of interest (ROI) was drawn (1030 um^2) either in the mPFC region or in the center of the vector cloud. This ROI was determined by superimposing an image of the brain atlas at the stereotaxic coordinates of the targeted mPFC region. Then, each image was converted to an 8-bit image. Images were then manually thresholded (top 125, bottom 135) to create a binary overlay in which c-Fos positive nuclei were covered and the background was minimized (Bernstein et al. 2019; Bal et al. 2020). Cells that were c-Fos positive, uniformly round, and of equal size

were selected manually and counted by the cell-count function (raw count) (Bal et al. 2020).

Statistical analysis

Data were analyzed using GraphPad Prism 10.2.2 software. To evaluate novelty preference (i.e. the interaction time DRs) a combination of hypothesis testing and estimation statistics were used. For all behavioral analyses, the entire 5 min of the sample or test phase was analyzed. Total stimuli exploration times were calculated by taking the sum of the time spent interacting with each stimulus, as measured in seconds. For all experiments, to evaluate novelty preference against chance, one-sample t-tests against 0 were used. Total exploration times were recorded as the total duration of interaction with all items during the sample or test phase. P values that were < or = to 0.05 were considered significant. In the first experiment, 2-way ANOVAs were used to evaluate the measures generated by the fiber photometry data. Tukey's Honest Significant Difference was performed as a post hoc test when significant main effects were observed. Unpaired t-tests were used to compare interaction bout measurements between tests (IST, DST). Tests were not included if the rat had insufficient exploration of all stimuli in either phase, if there was excessive noise in the fiber photometry signal, or if the fiber photometry cord was bent. In the second experiment, 2-way ANOVAs were performed with factors of Treatment (Saline, 1.0 mg/kg C21) and Sex (Male, Female). In the third experiment, a 3-way ANOVA with factors of Treatment (Saline, 1.0 mg/kg C21), Vector (Control, Active) and Test (IST, DST) was performed. Exploratory 2-way ANOVAs were also performed using a combination of the same factors. To follow up hypothesis testing, estimation statistics were performed to evaluate the magnitude of the effect sizes present using Cohen's d. Data are available by request.

Results

Increased activity in mPFC CaMKII-expressing neurons is necessary for novelty recognition under a higher memory load in the DST with odors

Odor-based incidental memory was measured in the spontaneous IST and DST tests with odors that measure novelty preference across low- and high-memory loads. A benefit of these spontaneous tests is that a variety of exploration and interaction behaviors can be measured. First, bout length and the number of visits to each stimulus was assessed to capture the patterns of interaction with stimuli throughout the tests. Male and female rats spent significantly more time with the novel item than with the familiar items in both the IST and DST tests with odors with no differences between the tests ($t(38) = 0.52$, $P = 0.61$) (Fig. 2A). Group means for the DR were well above a chance value of 0 (IST; $t(19) = 2.74$, $P = 0.013$; DST, $t(19) = 4.95$, $P < 0.001$), indicating a preference for the novel odor is both tests. No differences in the number of interactions were noted between the IST and DST tests with odors ($t(44) = 0.16$, $P = 0.87$) (Fig. 2B). However, rats had a significant increase in overall bout length in the DST compared to the IST with odors ($t(44) = 2.79$, $P = 0.0077$) (Fig. 2C). No differences were observed in the bout length of the first interaction with a stimulus in the sample phase of either test ($t(44) = 0.13$, $P = 0.89$) (Fig. 2D). Also, in the test phase, no differences were observed in the bout length of the first interaction with a novel stimulus ($t(44) = 1.23$, $P = 0.23$; Fig. 2E) or with a familiar ($t(44) = 0.73$, $P = 0.47$; Fig. 2F) stimulus between tests. This indicates that both male and female rats demonstrated novelty preference in the IST and DST with odors and spent more time overall interacting with stimuli in the DST.

Table 1. Summary of all interaction times for Figs. 3 and 4. The mean (± SEM) for the total interaction time seen with stimuli is recorded for each sample and test phase in the IST and DST with odors.

IST		DST	
Sample	**Test**	**Sample**	**Test**
44.89 ± 4.68	33.46 ± 2.78	48.63 ± 4.41	36.55 ± 3.14

Exploration times

When evaluating the total exploration times of the stimuli by the rats, no differences between the sample phases of the IST and DST were observed ($t(35) = 0.13$, $P = 0.89$) (Table 1). No differences were observed between the test phases of the IST and the DST ($t(35) = 0.73$, $P = 0.47$) (Table 1). As well, no differences were observed between sexes in the sample and test phases of the IST and DST ($F(7, 68) = 0.76$, $P = 0.62$). Thus, exploration times remained consistent regardless of phase, test, and sex.

Fiber photometry IST and DST sample phases

Here, fiber photometry was used to measure the calcium dynamics in CaMKII-expressing neurons in the mPFC of male and female rats during completion of the IST and DST with odors. In the following analysis we separate the data by the type of bout (Hackett et al. 2023). First, the z-scores of the "first bout" of interaction in the IST and DST are analyzed, by comparing the single values with t-tests. Next, we analyze the remaining "other bouts" of interaction in the IST and DST, by comparing the averaged z-scores in the IST and DST with t-tests. The first interaction with a stimulus in the sample phase is shown for both the IST and DST with odors (Fig. 3A). Heat maps show the z-scores for each rat's first interaction with stimuli in the IST (Fig. 3C) and the DST (Fig. 3D) with odors. The averaged z-scores of all the other interactions with stimuli during the sample phase of each rat is shown for the IST (Fig. 3E) and the DST (Fig. 3F) with odors. For each interaction with an odor stimulus in the sample phase, the area under the curve, peak z-score, peak frequency, and dynamic range was generated for the jGCaMP8m calcium signal. These values were averaged together for each type of interaction. In the sample phase of the IST and DST with odors, the first interaction with a stimulus (First) and the remaining other interactions (Other) were analyzed using paired t-tests. Interactions with stimuli for the first time in the DST with odors had a significantly higher averaged area under the curve ($t(18) = 2.05$, $P = 0.05$; Fig. 3G) and peak Z-score ($t(18) = 2.25$, $P = 0.037$; Fig. 3H), when compared to the IST with odors. No differences were also observed in the averaged peak frequency ($t(18) = 1.89$, $P = 0.07$; Fig. 3I) or in dynamic range ($t(18) = 0.34$, $P = 0.73$; Fig. 3J). When examining the averaged z-scores of the other interactions during the sample phases of the IST and DST with odors, no differences were observed in the area under the curve ($t(18) = 0.21$, $P = 0.83$; Fig. 3G), peak Z-score ($t(18) = 1.10$, $P = 0.29$; Fig. 3H), peak frequency ($t(18) = 0.39$, $P = 0.70$; Fig. 3I), or in dynamic range ($t(18) = 1.41$, $P = 0.18$; Fig. 3J). The consistent peak frequency and dynamic change indicates that there were no differences in the range of fluorescence intensity detected. The significantly higher peak z-score and area under the curve indicates that there is a greater response and sustained increase in mPFC neuronal activity during interaction with a stimulus for the first time in the sample phase of the DST than the IST with odors, as can be seen in Fig. 3A.

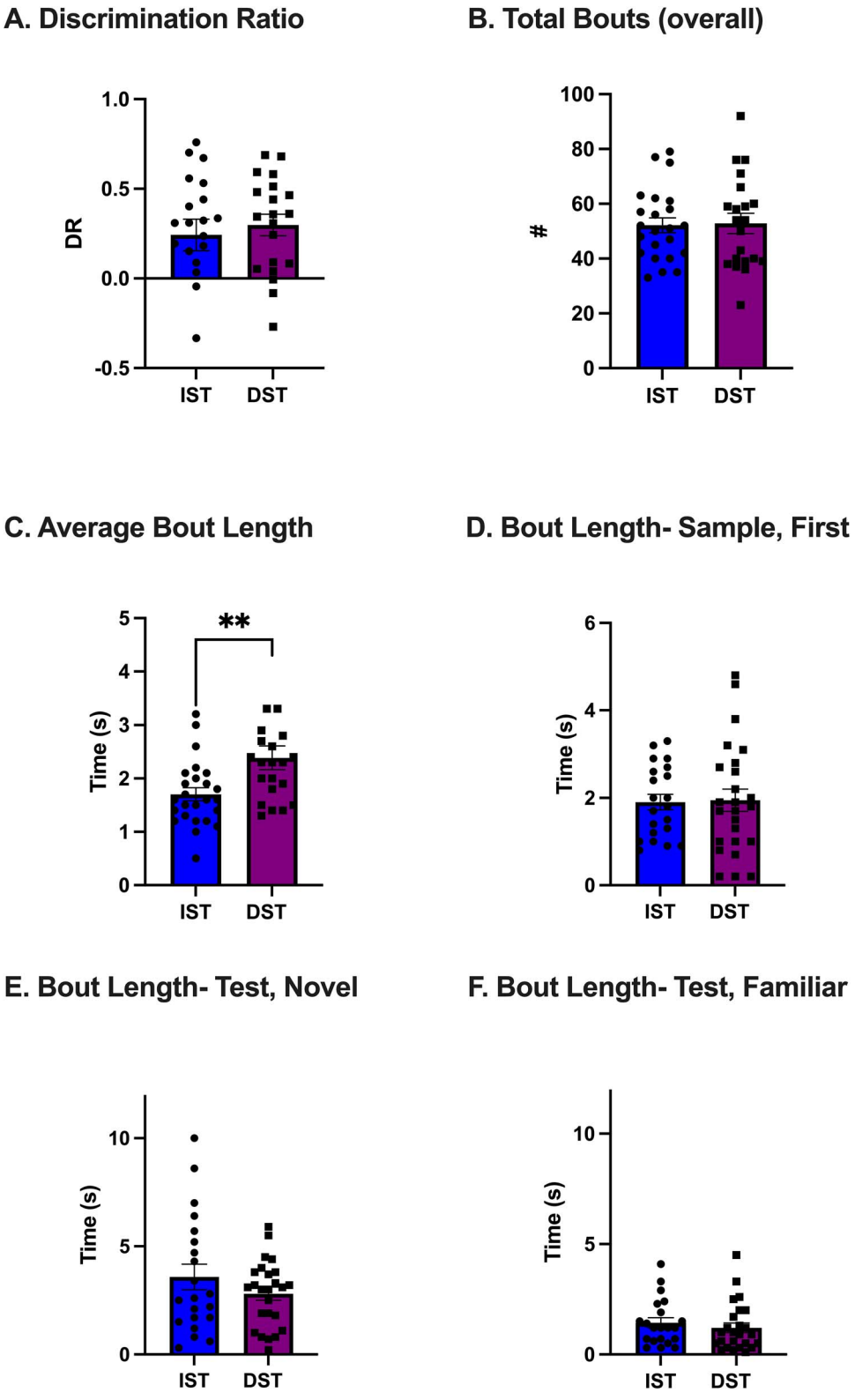

Fig. 2. No differences in bout duration between the IST and DST with odors. Rats demonstrated novelty preference in both the IST and DST with odors, performing well above chance (A). No differences in the overall number of bouts (B) are seen, but rats spent more time interacting with stimuli during the DST with odors (C). Rats also spent a similar amount of time interacting with an odor stimulus for the first time in the sample phase of the IST and DST with odors (D). In the test phase, no difference in the bout length is observed during the first visit to either a novel (E) or familiar (F) stimulus between tests. Bar graphs display the mean ± SEM. $^{**}P < 0.01$.

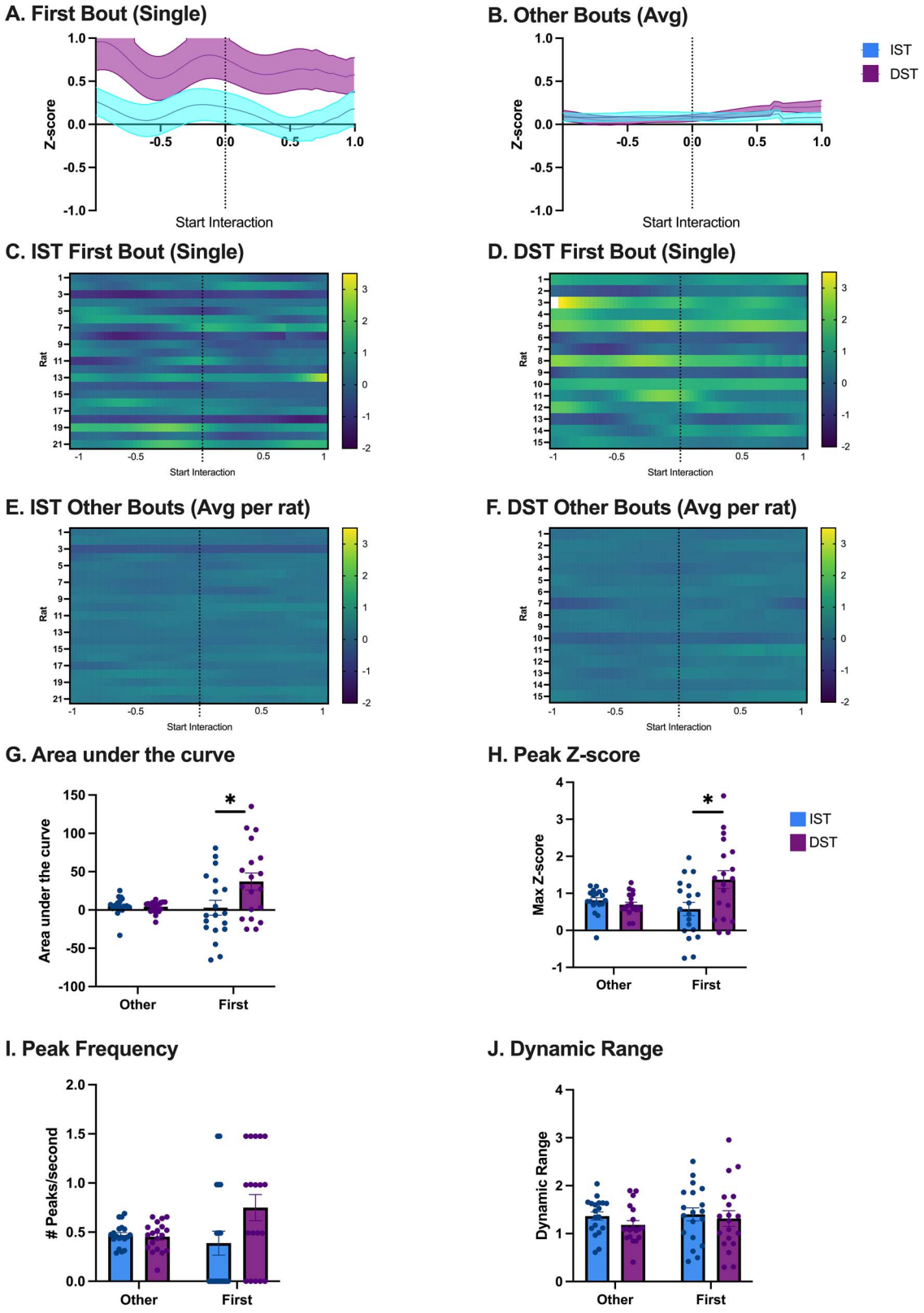

Fig. 3. Increased neuronal activity in the mPFC is observed in the sample phase of the DST with odors. The first bout with a stimulus (A) in the sample phase is shown by itself, and the average of all other bouts during the sample phase is shown separately (B). An increase in the z-score can be seen in the first interaction with a stimulus during the sample phase of the DST with odors in comparison to the IST with odors (A). Heat maps show the z-scores of the first interaction with a stimuli from each rat in the IST (C) and the DST (D) with odors. As well, the averaged z-scores of all the other interactions with stimuli during the sample phase of each rat is shown for the IST (E) and the DST (F) with odors. No specific patterns of activity emerge when looking at all the interactions averaged together. A significant increase is observed in the area under the curve during interaction with the first stimulus in the sample phase of the DST with odors in comparison to all other interactions in the DST and IST with odors (G). Similarly, the first interaction with a stimulus in the sample phase of the DST with odors has an increased peak Z-score in comparison to all other interactions in the DST and IST with odors (H). There was also no difference observed in the peak frequency during the sample phase of either the IST or DST with odors when interacting with stimuli (I). Lastly, no difference observed in the dynamic range during the test phase of either the IST or DST with odors when interacting stimuli (J). Bar graphs display the mean ± SEM. *$P < 0.05$.

Fiber photometry IST and DST test phases

Here, we also separate the data by the type of bout (Hackett et al. 2023). First, the averaged z-scores of "novel bouts" of interaction in the IST and DST are analyzed, by comparing the averaged values with t-tests. Next, we analyze the "familiar bouts" of interaction in the IST and DST, by comparing the averaged z-scores in the IST and DST with t-tests. The averaged z-scores of all the interactions with the familiar (Fig. 4A) and novel (Fig. 4B) stimuli in the test phase is shown for the IST and the DST with odors. Heat maps show the averaged z-scores of all the interactions with familiar stimuli during the test phase of each rat in the IST (Fig. 4C) and the DST (Fig. 4D) with odors. The averaged z-scores of all the interactions with novel stimuli during the test phase of each rat is also shown for the IST (Fig. 4E) and the DST (Fig. 4F) with odors. Here, a slight increase in activity can be observed during interactions with novel stimuli for some of the rats, but not all (Fig. 4F). For each interaction with an odor stimulus in the test phase, the area under the curve, peak z-score, peak frequency, and dynamic range was generated for the jGCaMP8m calcium signal. These values were averaged together for each type of interaction. In the test phase of the IST and DST with odors, the interactions with familiar (F) and novel (N) stimuli were analyzed using t-tests. Interactions with novel stimuli in the test phase of the DST with odors had a significantly higher averaged area under the curve ($t(33) = 2.45$, $P = 0.02$; Fig. 4G) and peak z-score ($t(33) = 2.28$, $P = 0.029$; Fig. 4H), when compared to the IST with odors. No differences were also observed in the averaged peak frequency ($t(33) = 1.28$, $P = 0.21$; Fig. 4I) or in dynamic range ($t(33) = 1.24$, $P = 0.22$; Fig. 4J). When examining the interactions with familiar stimuli in the test phases of the IST and DST with odors, no differences were observed in the area under the curve ($t(33) = 1.91$, $P = 0.065$; Fig. 4G), peak z-score ($t(33) = 1.24$, $P = 0.23$; Fig. 4H), peak frequency ($t(33) = 1.97$, $P = 0.06$; Fig. 4I), or in dynamic range ($t(33) = 1.33$, $P = 0.19$; Fig. 4J).The consistent peak frequency and dynamic change indicates that there were no differences in the range of fluorescence intensity detected. The significantly higher area under the curve indicates that there is a sustained increase in mPFC neuronal activity during interaction with a novel stimulus during the test phase of the DST, as can be seen in Fig. 4B.

C21 did not influence performance of the spontaneous incidental memory tests

Next, we used chemogenetics to precisely modulate neural activity in a targeted neuronal population. This less invasive approach allowed us to examine the effects of inhibiting CaMKII-expressing neurons in the mPFC in the odor-based incidental memory tests. First, we examined if the agonist used to activate the DREADD receptors had any effect on novelty preference in the IST and DST tests with odors.

In this experiment, the impact of the DREADD agonist C21 (1.0 mg/kg; i.p.) on IST and DST with odors performance in naïve, adult, male and female rats was tested when administered 1 h prior to completing the tests. In the IST with odors, there were no main effects of Sex ($F(1, 32) = 0.12$, $P = 0.73$) or Treatment ($F(1, 32) = 0.86$, $P = 0.36$), and no interaction ($F(1, 32) = 0.042$, $P = 0.84$) on novelty discrimination (Fig. 5C). In the DST with odors, there were also no main effects of Sex ($F(1, 32) = 0.74$, $P = 0.40$) or Treatment ($F(1, 32) = 0.29$, $P = 0.59$), and no interaction ($F(1, 32) = 0.041$, $P = 0.84$) on novelty discrimination (Fig. 5C). After combining sexes, rats in all treatment conditions performed above chance (Saline-IST; $P < 0.0001$, Saline-DST; $P < 0.0001$, C21- IST; $P = 0.011$, C21-DST; $P = 0.044$). When evaluating the total exploration times in the sample phase, there was no effect of Treatment in either the IST ($t(34) = 1.66$, $P = 0.11$) or DST ($t(34) = 0.60$, $P = 0.55$) with odors (Table 2). As well, when evaluating the total exploration time in the test phase, there was no effect of treatment in either the IST ($t(34) = 1.41$, $P = 0.16$) or DST with odors ($t(34) = 1.71$, $P = 0.097$) with odors (Table 2). These data demonstrate that an injection of C21 does not influence novelty recognition or exploration times in the odor-based IST and DST. In addition, we also demonstrated, for the first time, that female rats can successfully perform the IST and DST tests with odors with no notable differences in performance compared to our previous data generated using male rats (Barnard et al. 2023).

Inhibiting CaMKII-expressing neurons in the mPFC impaired novelty recognition in the DST with odors

The role of the mPFC in the IST and DST tests with odors was examined by activating inhibitory DREADDs expressed in the mPFC with a CaMKII promoter (Active group). Rats that expressed the control vector in the mPFC are referred to as the Control group. One male and one female rat from the Active group were not included due to improper placement and/or inadequate vector expression (final $n = 22$).

Discrimination ratios

To evaluate novelty preference, a 3-way ANOVA with factors of Test (IST, DST), Vector (Control, Active), and Treatment (Saline, C21) was performed. There was a main effect of Test ($F(1, 22) = 5.07$, $P = 0.035$), but not of Vector ($F(1, 22) = 1.08$, $P = 0.31$), or of Treatment ($F(1, 22) = 1.15$, $P = 0.30$). There was a significant interaction between Test and Treatment ($F(1, 22) = 6.11$, $P = 0.022$) and Vector and Treatment ($F(1, 22) = 6.13$, $P = 0.021$), but not between Test and Vector ($F(1, 22) = 1.91$, $P = 0.18$). There was also no interaction between Test, Vector and Treatment ($F(1, 22) = 0.41$, $P = 0.53$). Post hoc analyses revealed that rats with the active vector showed a significant decrease in novelty preference following an i.p. injection of C21 in the DST with odors, compared to rats with the control vector in the IST with odors ($P = 0.0067$).

Two exploratory ANOVAs were then performed to evaluate novelty preference in the IST and DST with odors separately with factors of Vector (Control, Active) and Treatment (Saline, C21). In the IST with odors, there was no main effect of Vector ($F(1, 36) = 2.51$, $P = 0.12$) or of Treatment ($F(1, 36) = 0.74$, $P = 0.40$), with no Interaction ($F(1, 36) = 1.59$, $P = 0.22$). In the DST with odors, there was no main effect of Vector ($F(1, 36) = 0.34$, $P = 0.56$) or an Interaction ($F(1, 36) = 2.35$, $P = 0.13$), but there was a main effect of Treatment ($F(1, 36) = 8.35$, $P = 0.0065$). Inspection of the data revealed that rats treated with C21 had significantly lower DRs, regardless of Vector. Further analysis showed that rats performed above chance in the IST with odors in both the Control vector group (Saline; $P = 0.012$, C21; $P = 0.0001$) and in the Active vector group (Saline; $P = 0.0002$, C21; $P = 0.028$) (Fig. 6A, 6B). As well, in the DST with odors, rats performed above chance in the Control vector group (Saline; $P = 0.0037$, C21; $P = 0.010$), but only following the *i.p.* injection of saline in the Active vector group (Saline; $P < 0.0001$, C21; $P = 0.082$) (Fig. 6A, 6B).

To build upon the hypothesis testing, estimation statistics were then used investigate the magnitude of the effect sizes between the various treatments. The first comparison evaluated the effect sizes between treatments within the IST and DST with odors. A small, non-significant effect size was observed between the treatment groups in the IST with odors [$d = 0.23$, 95% CI (−0.34, 0.81), $P = 0.44$]. In the DST with odors, a significant

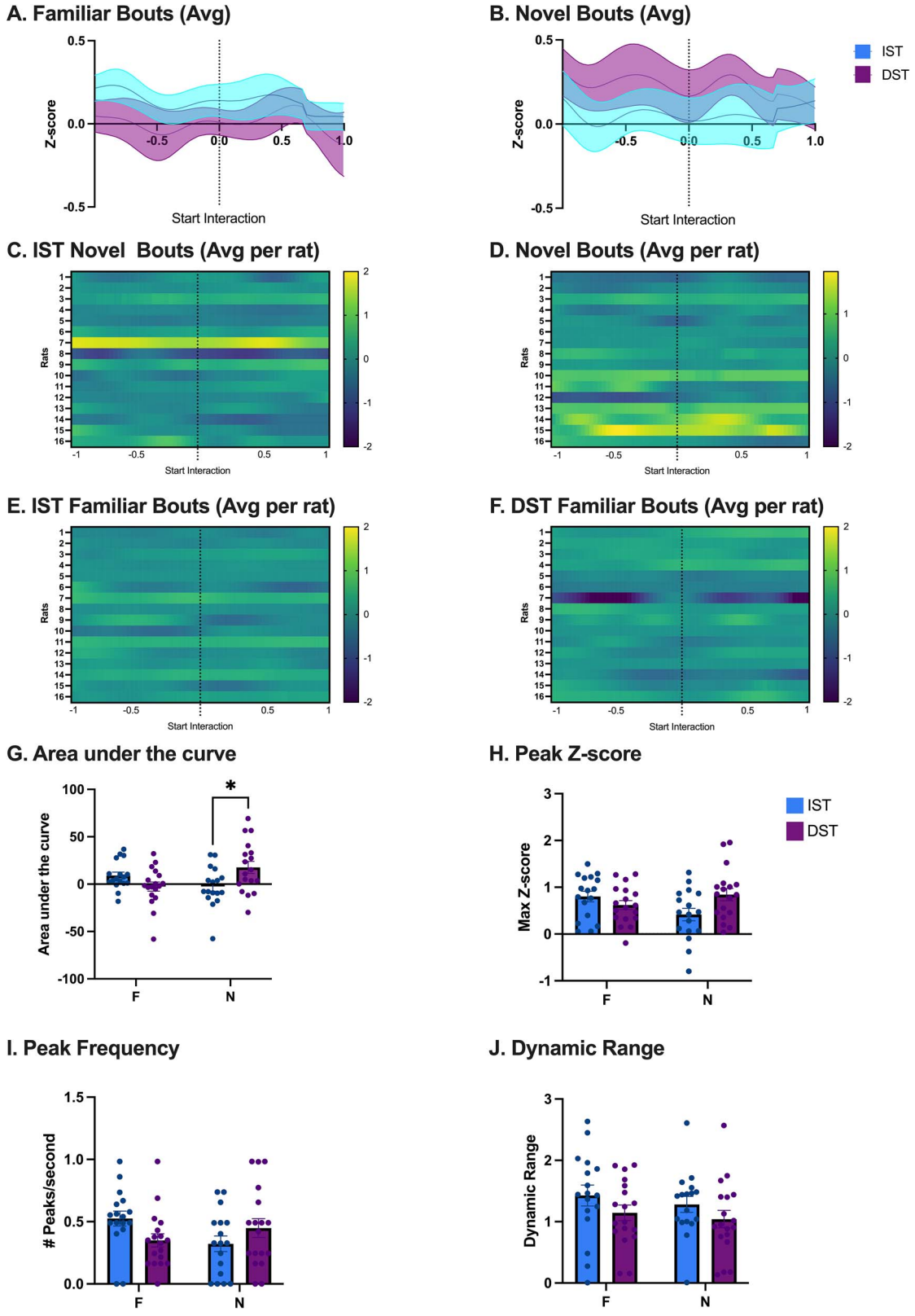

Fig. 4. Increase in mPFC neuronal activity during interaction with a novel stimulus in the test phase of the DST with odors. The average of all the interactions with the familiar (A) and novel (B) stimuli in the test phase is shown for the IST and the DST with odors. An increase in the averaged z-scores is seen during interactions with novel stimuli in DST with odors in comparison to the IST with odors (B). Heat maps show the averaged z-scores of all the interactions with familiar stimuli during the test phase of each rat in the IST (C) and the DST (D) with odors. As well, the averaged z-scores of all the interactions with novel stimuli during the test phase of each rat is shown for the IST (E) and the DST (F) with odors. A significant increase in the area under the curve during interaction with the novel stimulus in the test phase of the DST with odors in comparison to interaction with the novel stimulus in the test phase of the IST with odors (G). No notable differences are observed in the peak Z-score during the test phase of either the IST or DST with odors when interacting with either familiar or novel stimuli (H). There was also no difference observed in the peak frequency during the test phase of either the IST or DST with odors when interacting with either familiar or novel stimuli (I). Lastly, no difference observed in the dynamic range during the test phase of either the IST or DST with odors when interacting with either familiar or novel stimuli (J). Bar graphs display the mean ± SEM. *$P < 0.05$.

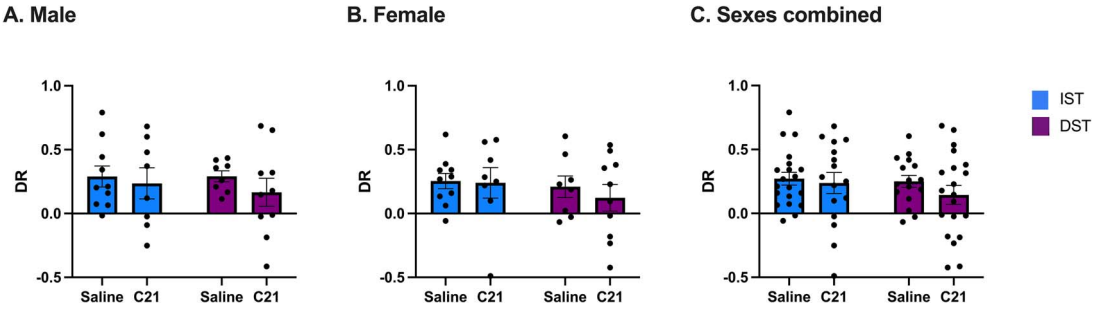

Fig. 5. Compound 21 (C21) does not significantly affect novel odor preference in the IST or DST with odors. Naïve adult male (A) and female (B) rats was tested. There was no observed difference in novelty preference between saline or C21 treatment conditions in either sex, or when samples were combined (C).

Table 2. Summary of all interaction times for Fig. 5. The mean (± SEM) for the total interaction time seen with stimuli is recorded for each sample and test phase in the IST and DST with odors following both an *i.p.* injection of saline and 1 mg/kg C21.

	IST		DST	
	Sample	**Test**	**Sample**	**Test**
Saline	48.99 ± 2.09	44.11 ± 3.25	46.68 ± 2.41	36.65 ± 2.24
C21 (1.0 mg/kg)	44.19 ± 1.99	38.11 ± 2.46	48.76 ± 2.46	42.18 ± 2.29

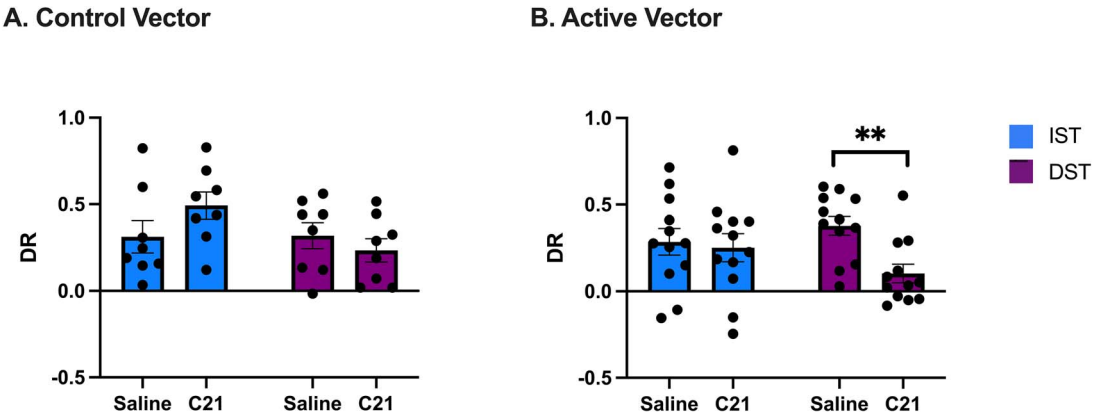

Fig. 6. Role of the mPFC in the IST and DST with odors. Rats performed the IST and DST with odors following both a saline and C21 *i.p.* injection (1 mg/kg). A discrimination ratio (DR) was generated to evaluate novelty preference (DR closer to 1). In the IST, there was no difference in novelty preference following the two treatments in rats with either the control vector (A) or the active vector (B) expressed in the mPFC. In the DST with odors, there was no difference in novelty preference following the two treatments in rats with the control vector (A) expressed in the mPFC. However, there was a significant decrease following an *i.p.* injection of C21 (1.0 mg/kg) in the rats with the active vector (B) expressed in the mPFC. This indicates a role for the mPFC in supporting odor-based incidental memory under higher memory loads. $^{**}P < 0.01$.

large effect size [d = −0.85, 95% CI (−1.48, −0.24), $P = 0.0046$] was observed as there was a notable decrease observed following an *i.p.* injection of C21 in comparison to a saline injection. The second comparison evaluated the effect sizes between treatment groups in rats expressing the Active and Control vectors. A small, non-significant effect size was observed between the treatment groups in rats with the Control vector [d = 0.24, 95% CI (−0.42, 0.91), $P = 0.45$]. Whereas in rats with the Active vector a significant medium effect size was observed between the treatments [d = −0.60, 95% CI (−1.18, −0.045), $P = 0.029$], where the novelty preference was notably lower following an *i.p.* injection of C21 in comparison to a saline injection.

Exploration times

When evaluating the total exploration times of the items by the rats, no differences between Saline and C21-treatments were observed in either the sample ($t(18) = 0.43$, $P = 0.68$) or the test ($t(18) = 0.84$, $P = 0.41$) phase in the Control vector group in the IST with odors (Table 3). As well, no differences in exploration times were seen in the sample ($t(22) = 1.43$, $P = 0.17$) or the test ($t(22) = 1.79$, $P = 0.084$) phase between Saline and C21-treatments in the Active vector group in the IST with odors (Table 3). In the DST with odors, there was no difference in exploration times in the sample ($t(18) = 0.89$, $P = 0.38$) phase, but there was a significant difference in the test ($t(18) = 2.52$, $P = 0.022$) phase in the Control vector group (Table 3). Here, the rats that received the *i.p.* injection of 1 mg/kg C21 had a significantly higher overall exploration times. There were no differences in exploration times were seen in the sample ($t(22) = 1.05$, $P = 0.30$) or test ($t(22) = 1.24$, $P = 0.22$) phase in the Active vector group (Table 3). Thus, C21 does not consistently alter exploration times in these tests.

Activation of the hM4D(Gi) DREADD decreased the number of c-Fos positive cells in the mPFC following the DST with odors

Lastly, we examined c-Fos expression in the mPFC, an immediate early gene protein, that is an indicator of neuronal activity. To investigate if the hM4D(Gi)-expressing neurons were

Table 3. Summary of all interaction times for Fig. 6. The mean (± SEM) for the total interaction time seen with stimuli is recorded for each sample and test phase in the IST and DST with odors following both an *i.p.* injection of saline and 1 mg/kg C21.

	IST Control Vector		IST Active Vector		DST Control Vector		DST Active Vector	
	Sample	**Test**	**Sample**	**Test**	**Sample**	**Test**	**Sample**	**Test**
Saline	44.90 ± 2.86	32.74 ± 3.29	45.55 ± 8.77	42.79 ± 5.33	42.00 ± 2.57	29.74 ± 2.11	39.43 ± 3.76	35.96 ± 3.58
C21 (1.0 mg/kg)	42.24 ± 3.40	35.91 ± 1.91	31.50 ± 4.40	31.78 ± 3.03	47.98 ± 6.16	50.22 ± 7.86	44.80 ± 3.47	44.89 ± 6.22

inhibited by C21, a subset of sections were immunolabeled for c-Fos. An unpaired t-test was used to evaluate the effect of Treatment (saline, 1.0 mg/kg C21) on the number of c-Fos positive cells in the mPFC-based ROI. A significant decrease in the number of c-Fos positive cells following an *i.p.* injection of 1 mg/kg C21 was observed in comparison to following an *i.p.* injection of saline ($t(21) = 2.73$, $P = 0.013$) (Fig. 7A). When examining the percent change of c-Fos positive cells in the mPFC- based ROI in comparison to home cage controls were made. There was a significant decrease in the number of c-Fos positive cells following an *i.p.* injection of 1 mg/kg C21 compared to after an *i.p.* injection of saline ($t(21) = 2.74$, $P = 0.012$) (Fig. 7B). When using the vector cloud-based ROI, a decrease in the number of c-Fos positive cells following the i.p. injection of 1 mg/kg C21 was apparent, although it was not significant ($t(21) = 0.85$, $P = 0.41$) (Fig. 7A). The mPFC-based ROI was used in the main analysis, therefore the percent change of c-Fos positive cells was not calculated for the vector cloud-based ROI. When examining the representative images, a decrease in the number of DREADD expressing c-Fos positive cells can be seen following an *i.p.* injection of 1 mg/kg C21 compared to after an *i.p.* injection of saline (Fig. 7C, D).

Discussion

In this study, we found a unique sustained increase in mPFC neuronal activity during interaction with a novel stimulus under a higher memory load in the test phase of the DST with odors (Fig. 3). Consistent with a critical role of this increased activity for novelty preference in the DST, impaired novelty preference was observed in the DST with odors following C21, but not in the IST with odors, in rats expressing the hM4D(Gi) DREADD in the mPFC (Fig. 6). No impact on novelty preference in the IST or DST with odors was observed following either C21 or saline in naïve male or female rats (Fig. 5) or those expressing a control vector in the mPFC (Fig. 6). As well, a notable decrease in the number of c-Fos positive cells is observed in the mPFC following an injection of C21 activating the hM4D(Gi) DREADD (Fig. 7). These data indicate a necessary role of mPFC in supporting odor-based incidental memory under a higher memory load.

Ecological validity of the IST and DST

Spontaneous recognition tests boast high ecological validity, as rodents frequently encounter novel stimuli in the wild and use this information to navigate and interact with their environment. In mice, it has been shown using object versions of the IST and DST with three, four, six, and nine different objects that both male and female mice can remember up to six objects (Torromino et al. 2022). We have also previously shown that rats perform the IST and DST with both six objects and six odors, but the underlying circuitry supporting the odor-based tests is understudied (Barnard et al. 2023). Rats use olfaction to extract information about their environments. Items in their environments have olfactory signatures which increases the complexity of chemosensory processing (Rokni and Ben-Shaul 2024). In the IST and DST, single odor objects are used as the odor stimuli (each jar has a unique odor) and in the current testing apparatus, no barriers or separations exist between the different odor stimuli. As a result, there is the potential for interactions to occur between the different odor molecules, which introduces extrinsic variability (Rokni and Ben-Shaul 2024). As well, the different odor molecules have varying volatility and diffusion constants, and other factors within the testing environment like airflow and temperature can also impact the interactions between the odor molecules (Rokni and Ben-Shaul 2024). The differences in the sensory experiences in the IST and DST can provide an alternative explanation to memory load when considering differences in novelty preference and supporting brain regions. However, the lack of an effect observed following inhibition by the DREADD's in the IST (Fig. 6B) supports the idea that the mPFC supports increased memory load, as the sensory experience is similar in the two tests. In natural environments, no odor molecules exist in perfect isolation, which increases the ecological validity of tests like the IST and DST for examining rodent odor-based recognition memory. Further, these tests do not require a long training period, learned rules, food restriction, or considerable experimental involvement. The spontaneous and flexible design of the tests also allows for the testing of rodents across different ages and the ability to model a variety of diseases and disorders. Ultimately these tests boast high ecological validity, as rodents frequently encounter novel stimuli in the wild and use the various sensory information to navigate and interact with their environment.

Male and female rats demonstrate comparable novelty preference in the IST and DST with odors

These experiments also show that there were no observed differences for novelty preference on the IST and DST with odors between sexes, similar to data from our previous work (Black et al. 2025). In addition, in the DST with odors, both males and females spent more time interacting with stimuli in comparison to the IST with odors. This is consistent with observations made previously in our lab, showing that male and female rats have equivalent exploration times of objects during a variety of spontaneous recognition tests (McElroy et al. 2025). However, there is work that highlights sex differences in spatial processing and exploration strategies in rodents (McElroy and Howland, 2025; Levy et al. 2023; Becegato and Silva 2022; Kokras and Dalla 2014; Chow et al. 2013; Herlitz and Rehnman 2008). For example, females have increased locomotor and darting behaviors in a spontaneous object-in-place recognition memory test, whereas males moved slower and traveled less overall (McElroy and Howland, 2025). Although, despite some nuanced sex differences in how rats explore their environments, this does not seem to impact their overall novelty preference performance in spontaneous recognition-based tests (McElroy and Howland, 2025). The findings of this paper further

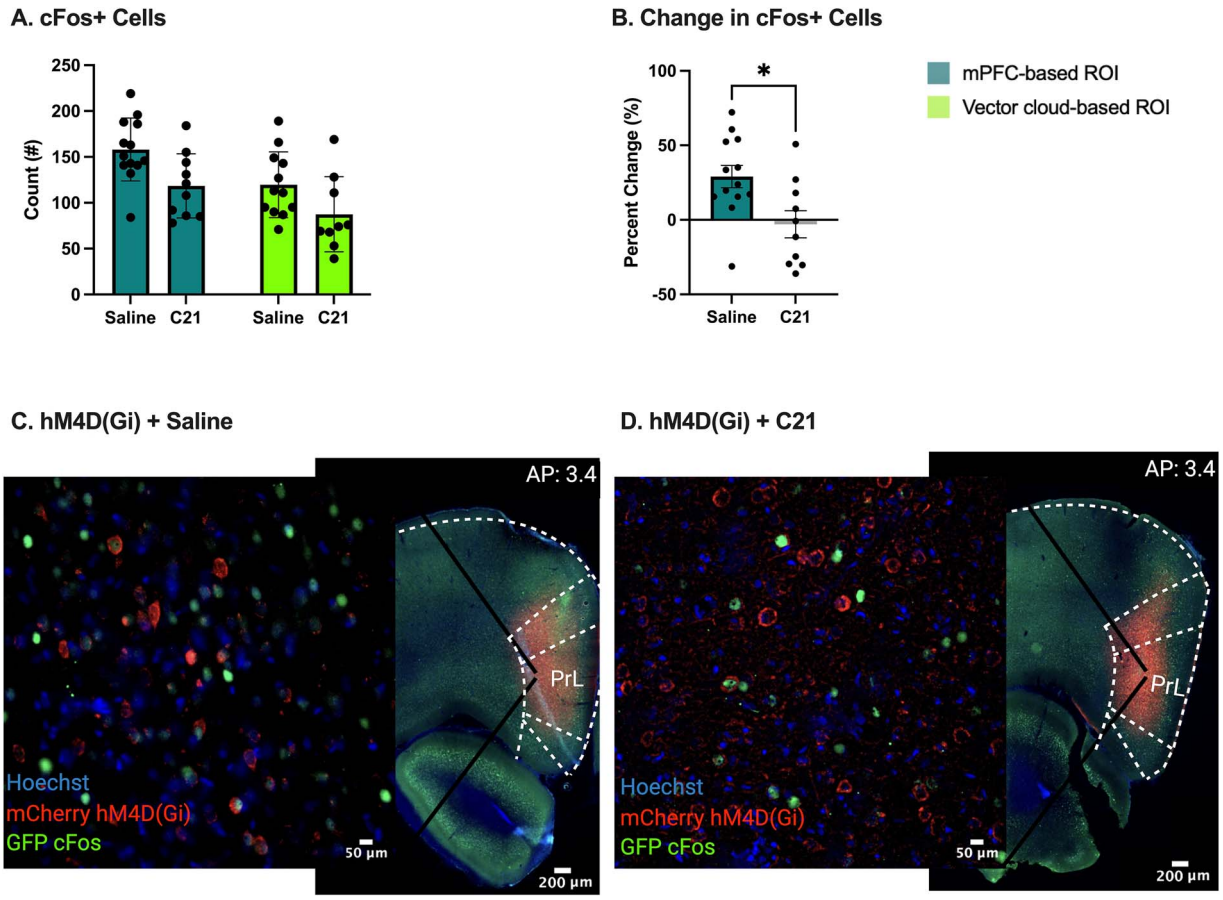

Fig. 7. Examining c-Fos as a biomarker for neural activity in the mPFC. Rats performed the DST with odors following either a saline and C21 *i.p.* injection (1 mg/kg) to activate the hM4D(Gi) DREADD expressed in the mPFC. (A) There was a decrease in the number of c-Fos positive cells in the mPFC- based ROI following an *i.p.* injection of C21. (A) There was also a significant increase in the number of c-Fos positive cells in comparison to home cage rats following exposure to the DST test when using the mPFC-based ROI for analysis. An *i.p.* injection of C21 prevented this increase. (B) A visual decrease, albeit not significant, is observed following an *i.p.* injection of C21 in the number of c-Fos positive cells in the vector cloud- based ROI. (C, D) As well, a visual decrease is observed following an *i.p.* injection of C21 in the number of colocalized cells. The prelimbic region of the mPFC (PrL) is labeled. $^{*}P < 0.05$.

support these previous observations, as comparable performance on the IST and DST with odors was observed between sexes.

The mPFC is necessary for encoding odor information and novelty recognition in the DST with odors

Using fiber cannulae implanted in the prelimbic region of the mPFC, we showed that neuronal activity differs between phases and between the IST and DST with odors (Figs. 3, 4). During the sample phase, no specific patterns of neuronal activity emerged in the IST or DST with odors, except for an increase in activity during the first visits to stimuli in the DST with odors (Fig. 3A). In the test phase of the DST with odors, we observed a sustained increase in mPFC neuronal activity during interaction with the novel stimulus compared to the familiar stimuli (Fig. 4B, F). During the IST with odors, although preferential interaction with the novel stimulus was observed from the DR's, no distinct patterns of neuronal activity in the mPFC emerge (Fig. 4A, E). These data indicate that the mPFC may play a unique role in helping to generate a novelty signal that subsequently influences novelty recognition under a higher memory load in the DST. These findings are in line with previous research demonstrating that the prelimbic region of the mPFC is critical for driving investigatory behavior involved in exploring stimuli (Ahmadlou et al. 2021). Ultimately, the prelimbic region of the mPFC processes and integrates the sensory information of the stimuli to then facilitate investigation of the stimuli that supports novelty preference.

The main olfactory pathway processes odor-based information by detecting and identifying odor molecules. However, depending on the type of odor information, different brain regions are involved in the use of this odor-based information. The mPFC is a highly interconnected brain region known to help integrate and orchestrate the use of odor-based information (Feinberg et al. 2012; Murphy and Deutch 2018; Mathiasen et al. 2023; Jun et al. 2024; Sauvage et al. 2010; Persson et al. 2022; Chao et al. 2016; Cansler et al. 2023). Specifically, the prelimbic region of the mPFC supports novelty preference, likely mediated by memory, in test paradigms that use social odors through connections with other cortical areas. The prelimbic region of the mPFC receives projections from the perirhinal cortex (Feinberg et al. 2012) and from the medial orbitofrontal cortex with information regarding the valence of the odor cues (Murphy and Deutch, 2018; Mathiasen et al. 2023). Importantly, the orbitofrontal cortex relays information from the insular cortex regarding gustatory and visceral sensory information to the mPFC (Mathiasen et al. 2023) as rats use their whiskers and sometimes bite the stimuli during an interaction. The prelimbic region also has bidirectional projections with the lateral entorhinal cortex which plays a critical role in forming odor-context associative memories (Sauvage et al. 2010; Chao et al. 2016; Persson et al. 2022; Jun et al. 2024) and

in rapid odor discrimination (Bitzenhofer et al. 2022). The lateral entorhinal cortex itself has many reciprocal connections with other olfactory regions like the olfactory bulb and piriform cortex, further supporting its role in olfactory memory processes (Xu and Wilson, 2013). Lastly, connections between the prelimbic region of the mPFC and the olfactory tubercle exist, which have been implicated in supporting odor-directed selective attentional processes which influence odor processing (Cansler et al. 2023). The above discussion highlights how the mPFC is a highly integrative region with various connections to and from a variety of brain regions involved in odor sensory and memory processes. In the DST with non-social odors, it is likely that the prelimbic region of the mPFC integrated information from the medial orbitofrontal cortex, the lateral entorhinal cortex, and the olfactory tubercle to support odor-based recognition.

It is important to note that in both the fiber photometry and chemogenetic experiments the vector was not restricted to the prelimbic region of the mPFC, though it was the intended target given some of the anatomical similarities to the human ventromedial PFC and functional similarities to the human dorsolateral PFC (Howland et al. 2022). The slight spread of the vector into the infralimbic region of the mPFC may have influenced the observed recognition memory deficits. A function of the infralimbic region of the mPFC is to support contingency learning, which is the process of learning the relationship between various stimuli and the outcome of behavioral responses and is implicated in recognition memory (Nett and LaLumiere 2021). The prelimbic and infralimbic regions of the mPFC do coordinate behavior in a complementary manner, as many excitatory connections exist between these regions (Marek et al. 2018). Therefore, given that the vector was contained within the mPFC region of the rat, and that the subregions play complimentary roles in supporting recognition memory, we discussed the results in reference to the rat mPFC.

Increased activity or certain patterns of activity in a particular population of neurons in areas like the lateral PFC of humans and primates has been thought to represent the information being held in working memory (Thrower et al. 2023). Using techniques like neurophysiological recordings and magnetic resonance imaging (MRI), studies have shown how the lateral PFC helps control the content and amount of the information held in working memory, and facilitates subsequent actions informed by this information (Kiyonaga et al. 2024; Tang et al. 2019: Thrower et al. 2023). Although the rat and human PFC's have anatomical differences, there are functional similarities between the human lateral PFC and the rat mPFC (Hoover and Vertes 2007; Euston et al. 2012; Howland et al. 2022). The results of this study highlight the role of the PFC in supporting short-term memory processes in rats, which are related to working memory processes in humans and primates.

Conclusions and future directions

Here we showed that CaMKII-expressing neurons in the mPFC are critical for novelty preference under a higher memory load in the odor-based DST. These data suggest that activity in CaMKII-expressing neurons in the mPFC is not necessary for performance on the IST with odors. This study also demonstrates an effective use of fiber photometry and chemogenetic techniques to record and manipulate neuronal activity in the mPFC. Together, these data indicate that the impairments in odor-based recognition memory were due to the selective and temporary inactivation of mPFC neurons. A future experiment could investigate the specific involvement of the projections between the orbitofrontal cortex or the lateral entorhinal cortex and the mPFC in odor-based recognition memory using a combination of vectors that encode site-specific DNA recombinase (Hui et al. 2022). This would ultimately allow for a more complete understanding of the neural substrates supporting odor-based novelty recognition.

Acknowledgements and funding sources

Funding for these experiments was obtained from the University of Saskatchewan College of Medicine and the Natural Sciences and Engineering Research Council of Canada (NSERC) to JGH. ILB was supported by a scholarship from NSERC. DLM was supported by scholarships from the University of Saskatchewan Colleges of Medicine and Graduate and Postdoctoral Studies. AEG and KMY were supported by scholarships from NSERC and the University of Saskatchewan College of Medicine. We thank Dr Olivia Hon at Neurophotometrics for her invaluable help and insight in setting up the fiber photometry system and in the early stages of data analysis.

Author contribution

Ilne L. Barnard (Conceptualization, Data curation, Formal Analysis, Investigation, Methodology, Writing—original draft, Writing—review & editing), Dan L. McElroy (Conceptualization, Investigation, Methodology, Validation, Writing—review & editing), Kaylen M. Young (Data curation, Formal Analysis), Dylan J. Terstege (Data curation, Formal Analysis, Methodology, Resources, Software, Visualization), Aiden E. Glass (Data curation, Formal Analysis, Investigation, Methodology), Jonathan R. Epp (Conceptualization, Formal Analysis, Methodology, Software, Supervision), Justin J. Botterill (Conceptualization, Formal Analysis, Methodology), John Howland (Conceptualization, Funding acquisition, Investigation, Methodology, Project administration, Supervision, Validation, Writing—original draft, Writing—review & editing).

Funding

None declared.

Conflict of interest statement: The authors of this study have no conflicts to declare.

References

Aggleton JP, Nelson AJD. 2020. Distributed interactive brain circuits for object-in-place memory: a place for time? *Brain Neurosci Adv*. 4:2398212820933471. https://doi.org/10.1177/2398212820933471.

Ahmadlou M et al. 2021. A cell type-specific cortico-subcortical brain circuit for investigatory and novelty-seeking behavior. *Science*. 372:eabe9681. https://doi.org/10.1126/science.abe9681.

Bal A, Maureira F, Arguello AA. 2020. SimpylCellCounter: an automated solution for quantifying cells in brain tissue. *Sci Rep*. 10:12570.

Barch DM, Smith E. 2008. The cognitive neuroscience of working memory: relevance to CNTRICS and schizophrenia. *Biol Psychiatry*. 64:11–17. https://doi.org/10.1016/j.biopsych.2008.03.003.

Barnard IL et al. 2023. High-THC cannabis smoke impairs working memory capacity in spontaneous tests of novelty preference for objects and odors in rats. *eNeuro*. 10:ENEURO.0115-23.2023. https://doi.org/10.1523/ENEURO.0115-23.2023.

Becegato M, Silva RH. 2022. Object recognition tasks in rats: does sex matter? *Front Behav Neurosci*. 16:970452. https://doi.org/10.3389/fnbeh.2022.970452.

Bernstein HL, Lu YL, Botterill JJ, Scharfman HE. 2019. Novelty and novel objects increase c-Fos immunoreactivity in mossy cells in the mouse dentate gyrus. *Neural Plast*. 2019:1815371.

Bitzenhofer SH, Westeinde EA, Zhang H-XB, Isaacson JS. 2022. Rapid odor processing by layer 2 subcircuits in lateral entorhinal cortex. *Elife*. 11:e75065. https://doi.org/10.7554/eLife.75065.

Black T et al. 2025. Differential effects of gestational Cannabis smoke and phytocannabinoid injections on male and female rat offspring behavior. *Prog Neuropsychopharmacol Biol Psychiatry*. 136:111241.

Botterill JJ et al. 2021. Off-target expression of Cre-dependent adeno-associated viruses in wild-type C57BL/6J mice. *eNeuro*. 8:ENEURO.0363-21.2021. https://doi.org/10.1523/ENEURO.0363-21.2021.

Botterill JJ et al. 2024. Dorsal peduncular cortex activity modulates affective behavior and fear extinction in mice. *Neuropsychopharmacology*. 49:993–1006. https://doi.org/10.1038/s41386-024-01795-5.

Broadbent NJ, Squire LR, Clark RE. 2004. Spatial memory, recognition memory, and the hippocampus. *Proc Natl Acad Sci USA*. 101:14515–14520. https://doi.org/10.1073/pnas.0406344101.

Broadbent NJ, Gaskin S, Squire LR, Clark RE. 2010. Object recognition memory and the rodent hippocampus. *Learn Mem*. 17:5–11.

Bussey TJ, Saksida LM, Murray EA. 2006. Perirhinal cortex and feature-ambiguous discriminations. *Learn Mem*. 13:103–105; author reply 106-7. https://doi.org/10.1101/lm.163606.

Cansler HL et al. 2023. Organization and engagement of a prefrontal-olfactory network during olfactory selective attention. *Cereb Cortex*. 33:1504–1526.

Cansler HL et al. 2023. Organization and engagement of a prefrontal-olfactory network during olfactory selective attention. *Cereb Cortex*. 33:1504–1526. https://doi.org/10.1093/cercor/bhac153.

Chao OY, Huston JP, Li J-S, Wang A-L, de Souza Silva MA. 2016. The medial prefrontal cortex-lateral entorhinal cortex circuit is essential for episodic-like memory and associative object-recognition. *Hippocampus*. 26:633–645. https://doi.org/10.1002/hipo.22547.

Chow C, Epp JR, Lieblich SE, Barha CK, Galea LAM. 2013. Sex differences in neurogenesis and activation of new neurons in response to spatial learning and memory. *Psychoneuroendocrinology*. 38:1236–1250. https://doi.org/10.1016/j.psyneuen.2012.11.007.

Davies DA, Molder JJ, Greba Q, Howland JG. 2013. Inactivation of medial prefrontal cortex or acute stress impairs odor span in rats. *Learn Mem*. 20:665–669. https://doi.org/10.1101/lm.032243.113.

De Falco E et al. 2019. The rat medial prefrontal cortex exhibits flexible neural activity states during the performance of an odor span task. *eNeuro*. 6:ENEURO.0424-18.2019. https://doi.org/10.1038/s41467-019-13740-y.

Du M, Santiago A, Akiz C, Aoki C. 2022. GABAergic interneurons' feedback inhibition of dorsal raphe-projecting pyramidal neurons of the medial prefrontal cortex suppresses feeding of adolescent female mice undergoing activity-based anorexia. *Brain Struct Funct*. 227:2127–2151. https://doi.org/10.1007/s00429-022-02507-9.

Eichenbaum H, Robitsek RJ. 2009. Olfactory memory: a bridge between humans and animals in models of cognitive aging. *Ann N Y Acad Sci*. 1170:658–663. https://doi.org/10.1111/j.1749-6632.2009.04012.x.

Ennaceur A. 2010. One-trial object recognition in rats and mice: methodological and theoretical issues. *Behav Brain Res*. 215:244–254. https://doi.org/10.1016/j.bbr.2009.12.036.

Ennaceur A, Aggleton JP. 1994. Spontaneous recognition of object configurations in rats: effects of fornix lesions. *Exp Brain Res*. 100:85–92. https://doi.org/10.1007/BF00227281.

Ennaceur A, Delacour J. 1988. A new one-trial test for neurobiological studies of memory in rats. 1: Behavioral data. *Behav Brain Res*. 31:47–59. https://doi.org/10.1016/0166-4328(88)90157-X.

Euston DR, Gruber AJ, McNaughton BL. 2012. The role of medial prefrontal cortex in memory and decision making. *Neuron*. 76:1057–1070. https://doi.org/10.1016/j.neuron.2012.12.002.

Farovik A, Dupont LM, Arce M, Eichenbaum H. 2008. Medial prefrontal cortex supports recollection, but not familiarity, in the rat. *J Neurosci*. 28:13428–13434. https://doi.org/10.1523/JNEUROSCI.3662-08.2008.

Feinberg LM, Allen TA, Ly D, Fortin NJ. 2012. Recognition memory for social and non-social odors: differential effects of neurotoxic lesions to the hippocampus and perirhinal cortex. *Neurobiol Learn Mem*. 97:7–16. https://doi.org/10.1016/j.nlm.2011.08.008.

Hackett J et al. 2023. Repeat investigation during social preference behavior is suppressed in male mice with prefrontal cortex cacna1c (Cav1.2)-deficiency through the dysregulation of neural dynamics. bioRxivorg:2023 June 24.546368. Accessed June 12, 2025. Available at:. https://doi.org/10.3390/sports12010014. http://dx.doi.org/10.1101/2023.06.24.546368 [

Herlitz A, Rehnman J. 2008. Sex differences in episodic memory. *Curr Dir Psychol Sci*. 17:52–56. https://doi.org/10.1111/j.1467-8721.2008.00547.x.

Hoover WB, Vertes RP. 2007. Anatomical analysis of afferent projections to the medial prefrontal cortex in the rat. *Brain Struct Funct*. 212:149–179. https://doi.org/10.1007/s00429-007-0150-4.

Howland JG, Ito R, Lapish CC, Villaruel FR. 2022. The rodent medial prefrontal cortex and associated circuits in orchestrating adaptive behavior under variable demands. *Neurosci Biobehav Rev*. 135:104569. https://doi.org/10.1016/j.neubiorev.2022.104569.

Hui Y et al. 2022. Strategies for targeting neural circuits: how to manipulate neurons using virus vehicles. *Front Neural Circuits*. 16:882366. https://doi.org/10.3389/fncir.2022.882366.

Jendryka M et al. 2019. Pharmacokinetic and pharmacodynamic actions of clozapine-N-oxide, clozapine, and compound 21 in DREADD-based chemogenetics in mice. *Sci Rep*. 9:4522.

Jun H et al. 2024. Prefrontal and lateral entorhinal neurons co-dependently learn item-outcome rules. *Nature*. 633:864–871. https://doi.org/10.1038/s41586-024-07868-1.

Kiyonaga A, Miller JA, D'Esposito M. 2024. Lateral prefrontal cortex controls interplay between working memory and actions. bioRxivorg Available at: http://biorxiv.org/lookup/doi/10.1101/2024 September 17.613601. Accessed June 22, 2025. https://doi.org/10.1101/2024September17.613601.

Kokras N, Dalla C. 2014. Sex differences in animal models of psychiatric disorders: sex differences in models of psychiatric disorders. *Br J Pharmacol*. 171:4595–4619. https://doi.org/10.1111/bph.12710.

Levy DR et al. 2023. Mouse spontaneous behavior reflects individual variation rather than estrous state. *Curr Biol*. 33:1358–1364.e4. https://doi.org/10.1016/j.cub.2023.02.035.

Marek R, Xu L, Sullivan RKP, Sah P. 2018. Excitatory connections between the prelimbic and infralimbic medial prefrontal cortex show a role for the prelimbic cortex in fear extinction. *Nat Neurosci*. 21:654–658. https://doi.org/10.1038/s41593-018-0137-x.

Mathiasen ML, Aggleton JP, Witter MP. 2023. Projections of the insular cortex to orbitofrontal and medial prefrontal cortex: a

tracing study in the rat. *Front Neuroanat*. 17:1131167. https://doi.org/10.3389/fnana.2023.1131167.

McElroy DL, Sabir H, Glass AE, Greba Q, Howland JG. 2024. The anterior retrosplenial cortex is required for short-term object in place recognition memory retrieval: role of ionotropic glutamate receptors in male and female long-Evans rats. *Eur J Neurosci*. 59: 2260–2275. https://doi.org/10.1111/ejn.16284.

McElroy DL et al. 2025. DREADD-mediated inhibition of anterior retrosplenial cortex: effects on novelty recognition of objects, locations, and object-in-place associations in male and female Long Evans rats. *Neurobiol Learn Mem*. 219:108055. https://doi.org/10.1016/j.nlm.2025.108055.

McElroy DL, Howland JG. 2025. Sex differences in exploratory behavior of rats successfully performing the object-in-place recognition memory test. *Behav Brain Res*. 477:115303.

Miranda JM, Cruz E, Bessières B, Alberini CM. 2022. Hippocampal parvalbumin interneurons play a critical role in memory development. *Cell Rep*. 41:111643. https://doi.org/10.1016/j.celrep.2022.111643.

Murphy MJM, Deutch AY. 2018. Organization of afferents to the orbitofrontal cortex in the rat. *J Comp Neurol*. 526:1498–1526. https://doi.org/10.1002/cne.24424.

Nett KE, LaLumiere RT. 2021. Infralimbic cortex functioning across motivated behaviors: can the differences be reconciled? *Neurosci Biobehav Rev*. 131:704–721. https://doi.org/10.1016/j.neubiorev.2021.10.002.

Olivito L et al. 2016. Phosphorylation of the AMPA receptor GluA1 subunit regulates memory load capacity. *Brain Struct Funct*. 221: 591–603. https://doi.org/10.1007/s00429-014-0927-1.

Olivito L, De Risi M, Russo F, De Leonibus E. 2019. Effects of pharmacological inhibition of dopamine receptors on memory load capacity. *Behav Brain Res*. 359:197–205. https://doi.org/10.1016/j.bbr.2018.10.041.

Persson BM et al. 2022. Lateral entorhinal cortex lesions impair odor-context associative memory in male rats. *J Neurosci Res*. 100: 1030–1046. https://doi.org/10.1002/jnr.25027.

Robinson S, Granata L, Hienz RD, Davis CM. 2019. Temporary inactivation of the medial prefrontal cortex impairs the formation, but not the retrieval of social odor recognition memory in rats. *Neurobiol Learn Mem*. 161:115–121. https://doi.org/10.1016/j.nlm.2019.04.003.

Rokni D, Ben-Shaul Y. 2024. Object-oriented olfaction: challenges for chemosensation and for chemosensory research. *Trends Neurosci*. 47:834–848. https://doi.org/10.1016/j.tins.2024.08.008.

Sannino S et al. 2012. Role of the dorsal hippocampus in object memory load. *Learn Mem*. 19:211–218. https://doi.org/10.1101/lm.025213.111.

Sauvage MM, Beer Z, Ekovich M, Ho L, Eichenbaum H. 2010. The caudal medial entorhinal cortex: a selective role in recollection-based recognition memory. *J Neurosci*. 30:15695–15699. https://doi.org/10.1523/JNEUROSCI.4301-10.2010.

Scott GA et al. 2020. Roles of the medial prefrontal cortex, mediodorsal thalamus, and their combined circuit for performance of the odor span task in rats: analysis of memory capacity and foraging behavior. *Learn Mem*. 27:67–77. https://doi.org/10.1101/lm.050195.119.

Tang H, Qi X-L, Riley MR, Constantinidis C. 2019. Working memory capacity is enhanced by distributed prefrontal activation and invariant temporal dynamics. *Proc Natl Acad Sci USA*. 116: 7095–7100. https://doi.org/10.1073/pnas.1817278116.

Terstege DJ et al. 2023. Protocol for the integration of fiber photometry and social behavior in rodent models. *STAR Protoc*. 4:102689. https://doi.org/10.1016/j.xpro.2023.102689.

Thrower L, Dang W, Jaffe RG, Sun JD, Constantinidis C. 2023. Decoding working memory information from neurons with and without persistent activity in the primate prefrontal cortex. *J Neurophysiol*. 130:1392–1402. https://doi.org/10.1152/jn.00290.2023.

Timme NM et al. 2022. Compulsive alcohol drinking in rodents is associated with altered representations of behavioral control and seeking in dorsal medial prefrontal cortex. *Nat Commun*. 13:3990.

Torromino G et al. 2022. Thalamo-hippocampal pathway regulates incidental memory capacity in mice. *Nat Commun*. 13:4194. https://doi.org/10.1038/s41467-022-31781-8.

Thompson KJ et al. 2018. DREADD Agonist 21 is an effective agonist for muscarinic-based DREADDs in vitro and in vivo. *ACS Pharmacol Transl Sci*. 1:61–72.

Unsworth N. 2016. Chapter One - The many facets of individual differences in working memory capacity. In: Ross BH, (eds). *Psychology of Learning and Motivation*. Volume 65. Academic Press: Cambridge, MA. p. 1–46.

Wagnon CC, Wehrmann K, Klöppel S, Peter J. 2019. Incidental learning: a systematic review of its effect on episodic memory performance in older age. *Front Aging Neurosci*. 11:173. https://doi.org/10.3389/fnagi.2019.00173.

Warburton EC, Brown MW. 2015. Neural circuitry for rat recognition memory. *Behav Brain Res*. 285:131–139. https://doi.org/10.1016/j.bbr.2014.09.050.

Xu W, Wilson DA. 2012. Odor-evoked activity in the mouse lateral entorhinal cortex. *Neuroscience*. 223:12–20.

Cerebral Cortex, 2025, **35**, bhaf203
https://doi.org/10.1093/cercor/bhaf203
Original Article